KINETIC STUDY OF THE THERMAL DECOMPOSITION OF LOW-GRADE NICKELIFEROUS LATERITE ORES

F. A. López[1,], M. C. Ramirez[2]; J. A. Pons[2], A. López-Delgado[1] and F. J. Alguacil[1]*

[1]Centro Nacional de Investigaciones Metalúrgicas (CSIC), Avda. Gregorio del Amo 8, Madrid 28040, Spain
[2]Instituto Superior Minero Metalúrgico, Las Coloradas s/n, Moa, Cuba

This study presents an evaluation of the decomposition kinetic of low-grade nickeliferous laterite by thermogravimetric analysis. Kinetic parameters were calculated using the Ozawa and the iso-conversional Friedman methods. Simplified kinetics models like those based on the reaction order were also applied for the simulations. Two-dimensional shrinkage models of the reaction interface mechanism were adopted as describing the thermal transformation process from non-isothermal kinetic analysis. The iso-conversional method (model-free kinetics) reveals that the decomposition of low-grade nickeliferous laterite does not follow a single mechanism because the determined activation energies and pre-exponential factor are not constant during the course of the reaction.

Keywords: goethite, kinetics, low-grade nickeliferous laterite ores, thermal decomposition

Introduction

Nickeliferous laterite ores reserves in the Republic of Cuba destined for nickel production are estimated at hundreds of millions of tons [1]. Cuban deposits include both high and low nickel content ores. The latter are concentrated in the upper strata of these deposits, immediately below the topsoil and are commonly known as 'low-grade nickeliferous laterite ores'; they are not used in nickel production since their Ni content does not reach the minimum input requirements of extraction plants. Depending on the deposit, the nickel content varies between 0.2 and 0.9% and also includes around 1.7% chromium and the mineralogical composition consists of goethite, maghemite and smaller amounts of hematite, chrome spinel, quartz and gibbsite. This ore possesses appreciable iron contents (45–55%) which allows its use in the iron and steel industry [2–4]. The presence in these materials of elements such as Ni, Cr and Co would allow their use for the production of special steels and ferroalloys [5, 6].

Most research on this material was focused on its characterisation and the application of extraction methods for the obtainment of different products [7], but not on studying its thermal decomposition. Thermal data is, however, of great interest in the planning of pyrometallurgical operations for the exploitation of this material. The literature includes numerous studies on goethite thermal analysis [8–15] but no references were found on the transformation kinetic of goethite in low-grade nickeliferous laterite ore.

This work studies the thermal decomposition kinetics of a low-grade nickeliferous laterite using thermogravimetric analysis techniques. Bearing in mind the mineralogical composition of this ore, the kinetics is based on the study of the goethite dehydroxylation reaction. Furthermore, this investigation compares the kinetics parameter obtained by the Ozawa method and advanced kinetic evaluation (differential iso-conversional Friedman analysis) of thermogravimetric curves and calculated by conventional methods, or the assumption of the reaction order.

Experimental

The sample was taken from low-grade ore at Zone A of Pedro Soto Alba Mine (Moa Nickel S.A.) at Moa (Cuba). The as-received sample (10 mm particle size) was grinded to a particle size of less than 0.83 mm. The average chemical composition, obtained by X-ray fluorescence analysis (Phillips PW 1410 spectrophotometer) is set out in Table 1. The crystalline phases detected by X-ray diffraction (Siemens D5000 diffractometer) were

Table 1 Chemical composition of low-grade nickeliferous laterites ores (expressed in mass% of oxides)

Compounds	Fe_2O_3	NiO	Co_3O_4	Cr_2O_3	Al_2O_3	SiO_2	MnO	ZnO	Total
Content/mass%	72.83	0.64	0.16	2.94	17.68	3.78	0.56	0.04	99.57

* Author for correspondence: flopez@cenim.csic.es
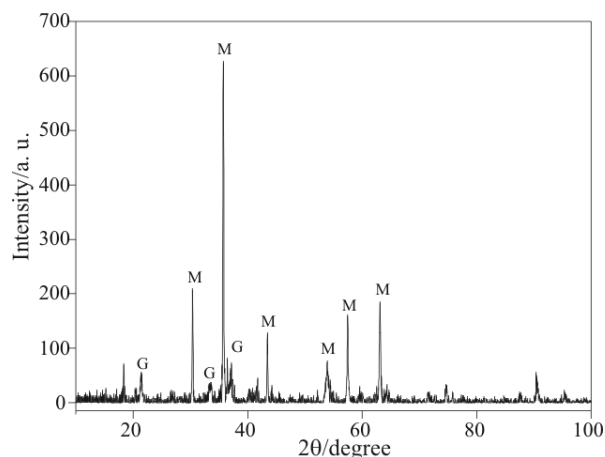
Fig. 1 X-ray pattern of initial low-grade nickeliferous ore (G=goethite, M=maghemite)

Fig. 2 DTA-TG curves for thermal decomposition of low-grade nickeliferous laterite ore (β=10 K min^{-1} in argon atmosphere)

maghemite (γ-Fe$_2$O$_3$), goethite (α-FeOOH) and lesser amounts of hematites (α-Fe$_2$O$_3$). Together with these major phases, small quantities of chrome spinel and quartz were found; the latter as opal and chalcedony (Fig. 1).

The DTA/TG curve was obtained at a heating rate of 10°C min^{-1} in argon atmosphere (20 mL min^{-1}) and using alumina crucibles (Setaram Setsys Evolution Model 1500). TG curves for kinetic studies (Shimadzu TGA 50H unit) were registered at heating rate varied between 5 and 30°C min^{-1}. The amount of sample used in each test was from 27 to 36 mg. The kinetic study was carried out on the basis of the derivative thermogravimetric (DTG) curves.

Kinetic parameters were evaluated by the isoconversional method, which involves determination of the temperatures corresponding to certain arbitrarily chosen values of the conversion extent α recorded in the experiments carried out at different heating rates β. Isoconversional methods are known as the Flynn and Ozawa methods [16, 17] and the Friedman method [18]. Kinetic parameters were also calculated by the ASTM E698 method [19]. The calculation method used in the model-free method was applied for simulations with AKTS-Thermokinetics software [20, 21] after baseline subtraction and normalisation of the exothermal peak obtained by different heating rates of low-grade nickeliferous laterite ores.

Results and discussion

DTA and TG results

Figure 2 shows the DTA/TG curves of the sample. Four main thermal effects are observed. The first, an endothermic effect at 100°C, corresponds to the elimination of water absorbed. The second corresponds to two consecutive endothermic peaks whose main peak appears at 305.5°C and corresponds to the
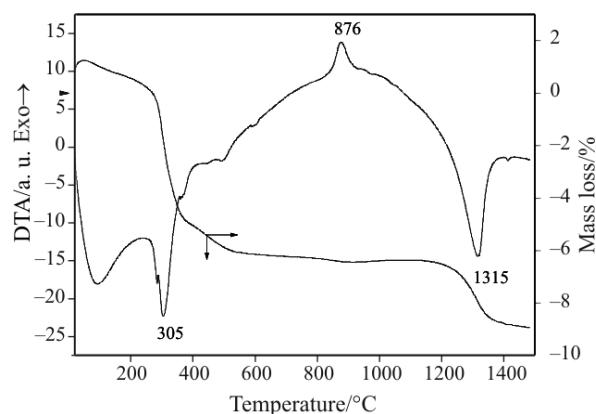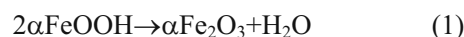
dehydroxylation of goethite which is transformed into hematite, in accordance with Eq. (1):

$$2\alpha FeOOH \rightarrow \alpha Fe_2O_3 + H_2O \qquad (1)$$

The appearance of this double effect in the dehydroxylation of goethite has previously been reported by Ghodsi *et al.* [22] and Schwertmann [23]. Several mechanisms of the solid-state transformation of goethite to hematite have been proposed. Both Watari *et al.* [24] and Goss [8] considered that the transformation proceeded by the direct dehydration of goethite to hematite without any intermediate phase. Özdemir and Dunlop [25] found that small amounts of magnetite were produced as an intermediate during the thermal transformation of goethite. Balek and Subrt [26] showed that during the thermal transformations important changes take place in the porosity and the morphology of the particles.

In the 375–500°C interval significant changes occur in the specific surface values determined by gas adsorption at the liquid nitrogen temperature. As can be seen in Fig. 2, the material continues to lose mass, although less sharply than in the previously analysed temperature range; here the losses do not exceed 1%, after which they remain practically invariable. In this temperature interval γ-Fe$_2$O$_3$ is transformed into α-Fe$_2$O$_3$. Figure 3a shows the diffractogram of the sample obtained after heating to 600°C. The appearance of hematite can be seen as a product of the complete dehydroxylation of goethite and of the partial transformation of maghemite into hematite. At temperatures above 720°C the higher mobility of atoms in the crystal lattice leads the activation energy to increase. This increased mobility causes the loss of hematite particle shape anisotropy and the interparticle sintering and a further decrease in the surface area observed. In the 720–850°C region the intensive agglomeration and interparticle sintering in the
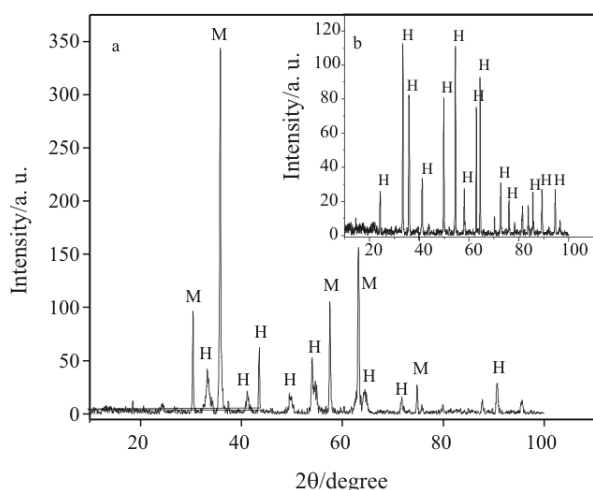
Fig. 3 Diffraction pattern of samples a – obtained after treatment at 600°C and b – after treatment at 1350°C (H=hematite, M=maghemite)

sample occur at approximately 850°C, resulting in the formation of large α-Fe_2O_3 particles of an irregular shape. This phenomenon is observed in the DTA curve through the appearance of the exothermic peak at 876.2°C. This peak does not have any associate mass loss, as is characteristic in recrystallisation phenomena. Finally, between 1200–1400°C a mass loss of 2.42% is observed on the TG curve, with an endothermic effect appearing at 1215°C on the DTA curve. This endothermic effect is due to the complete crystallisation of the hematite, as demonstrated in Fig. 3b, which shows the diffractogram of the sample obtained after heating to 1350°C, it being observed that the only crystalline mineralogical phase is hematite.

The total mass loss is 7.99% in the 20–1000°C range and 10.41% in the 20–1400°C range. These values are somewhat lower than those reported in the literature for laterites from this zone, whose mass loss values are between 12–18% in the 100–1000°C range [27].

Kinetic results

Table 2 displays TG data of the low-grade ore in the 30–1450°C range at different heating rates between 5-30°C min^{-1}.

Ozawa method

Figure 4 presents a graphic representation of ln β as a function of $1/T$ in the 0.9<α<0.1 range. It is seen that parallel straight lines are obtained, which means that for the analysed conversion grades the activation energy values will be close to each other. Table 3 displays the E values calculated from the slopes of the straight lines appearing in Fig. 4. In the analysed α value interval the activation energy remains practi-

Table 2 TG results of goethite dehydroxylation reaction

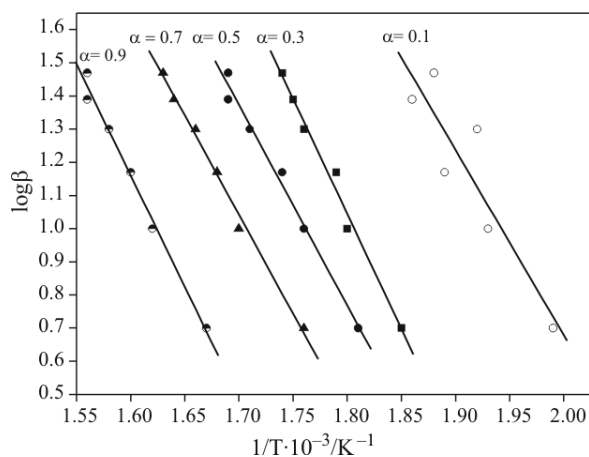| Heating rates (β)/°C min^{-1}	T_p/°C	Mass loss/%
5	272.6	5.55
10	289.3	5.36
15	297.5	5.50
20	303.1	5.55
25	314.0	5.47
30	317.0	5.42

(T_p=peak temperature)

Fig. 4 Ozawa plot

cally constant, yielding an average value of 114.40 kJ mol^{-1}±7.62. The kinetic model is fitted to the equation R_n: $n(1-\alpha)^{1-1/n}$. The best fit is obtained for n=2, implying two-dimensional shrinkage of the reaction interface mechanism. The pre-exponential coefficient is A=1.1·10^{10} s^{-1}.

The TG signals after correction of the baseline were used to estimate the reaction progress. The obtained α–T values were applied to calculate the kinetic parameters E and A, either by the non-isoconversional method of Friedman or by the simplified method, in which the function $f(\alpha)$ has been arbitrarily assumed to be in the form of the equation describing the autocatalytic, deceleratory α–T curves (R_n), diffusion mechanisms (D_n), sigmoidal α–T curves (Avrami–Erofeev models) and/or based on the reaction 'order' (F_n) [27]. The kinetic parameters were also calculated by the

Table 3 Activation energy obtained by Ozawa plot

Transformation degree, α	E/kJ mol^{-1}	R	SD
0.1	105.44	0.90776	0.1335
0.3	124.97	0.99293	0.0377
0.5	112.50	0.99374	0.0355
0.7	110.29	0.99669	0.0026
0.9	118.82	0.99493	0.02

(R=regression; SD=standard deviation)

Table 4 Activation energy and pre-exponential factor for goethite calculated from DTG signals by assuming commonly applied simplified reaction models

Reaction models	E/kJ mol^{-1}	A/s^{-1}	n	m
F_n: $(1-\alpha)^n$	111.8	9.32 107	1.24	–
F1: $1-\alpha$	91.67	1.19 106	1	–
F2: $(1-\alpha)^2$	176.83	1.42 108	2	–
Autocatalytic: $(1-\alpha)^n \alpha^m$	81.47	2.27 105	1.17	0.28
An: $n(1-\alpha) [-\ln(1-\alpha)]^{1-1/n}$	63.91	3.46 103	1.3	–
A1.5: $1.5 (1-\alpha) [-\ln(1-\alpha)]^{1/3}$	52.04	278	1.5	–
A2: $2 (1-\alpha) [-\ln(1-\alpha)]^{1/2}$	32.23	3.9	2	–
R2: $2 (1-\alpha)^{1/2}$	49.10	57	2	–
R3: $3 (1-\alpha)^{2/3}$	63.29	829	2	–
ASTM E698	123.66	4.818	3	–

standard ASTM E698 method. The results of the calculation of activation energy values by these simplified methods are presented in Table 4.

Model-free

It is worth mention here that the goethite dehydroxylation process is characterised by one activation value which certainly decreases significantly the accuracy of the lifetime predictions. The DTG signals of the studied samples are presented in Fig. 5 in the form of the dependence of the normalised heat flow on the temperature for five heating rates. The kinetic parameters calculated from the DTG plots allow the simulation of the reaction progress at any heating rate. Comparison of the experimental (symbols) with the simulated course of the reactions (lines) indicates a very good fit when the advanced kinetics analysis was applied.

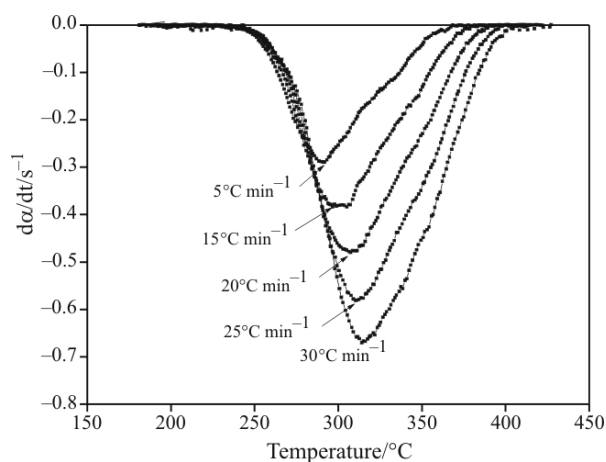The application of simplified kinetics (arbitrary assumption of the reaction mechanism) does not allow

the correct simulation of the experimental results. The trial simulations of the experimental decomposition course of goethite in a low-grade nickeliferous laterite ore sample applying the simplified models assuming an autocatalytic reaction model (a), F_n^{th} reaction model (b) and R_n reaction model (c). The results indicated that the commonly used method of the prediction of reaction rates based on the assumption of constancy of the reaction mechanism cannot lead to a proper description of the process. If the decomposition follows a single mechanism, then the reaction can be described in terms of a single pair of Arrhenius parameters and the commonly used set of reaction models. However, this approach is not acceptable for most of the decomposition reactions because, as presented in the Friedman analysis plot (Fig. 6), the activation energy is often strongly dependent on the reaction progress. The $d\alpha/dt$ conversion rates measured at different conversion extents of the kinetic parameter heating rates (straight lines in the diagrams) allowed the determination of the kinetic parameters A and E for the studied reactions as a function of the reaction extent presented in Fig. 7. It is seen that the activation energy over the whole of the dehydroxylation reaction is not constant. In the conversion grade interval $0<\alpha<1$, it varies between 122.2 and 103.5 kJ mol^{-1}.
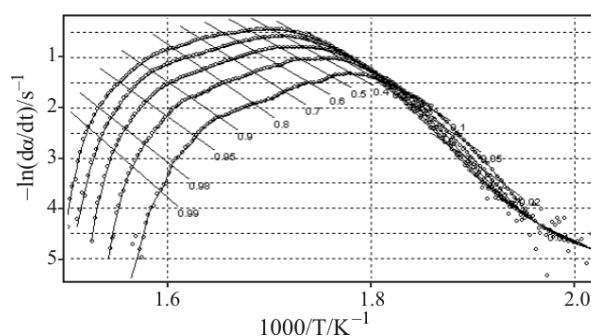

Fig. 5 Normalised DTG-signals as a function of temperature and heating rate. Experimental data is depicted as symbols, solid lines represent signals calculated on the basis of kinetic parameters derived from Friedman analysis

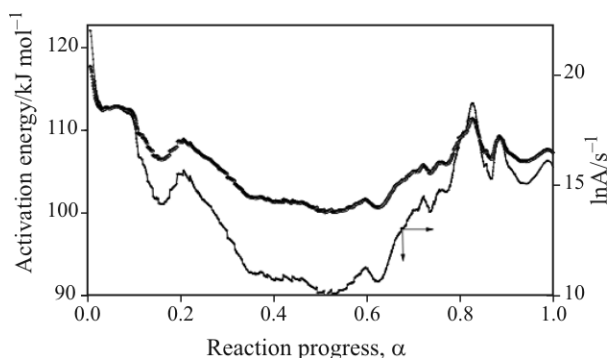**Fig. 6** Friedman analysis of goethite dehydroxylation

Fig. 7 Activation energy and pre-exponential factor as a function of reaction progress for goethite dehydroxylation

The pre-exponential factor varies between 22 and 10 s^{-1}.

Assuming a simple model for the goethite decomposition, the results obtained for the activation energy, 114.40 kJ mol^{-1} and the kinetic model (R_n for $n=2$) are similar to others found in the literature. Koga *et al.* [28], applying the Friedman method, studied the decomposition kinetics of a goethite obtained from $FeSO_4 \cdot 7H_2O$ solutions and subsequent hydrothermal treatment, as a function of particle size, in the $0.4 \leq \alpha \leq 0.95$ interval, obtaining activation energy values of between 137.4 and 142 kJ mol^{-1} and pre-exponential coefficient values between $1.50 \cdot 10^{-10}$ and $2.8 \cdot 10^{-10}$ s^{-10}. The thermal decomposition kinetics of the smallest particle size was expressed by the An equation $n(1-\alpha)[-\ln(1-\alpha)]^{1-1/n}$, indicating the nucleation and growth type mechanism. The R_n $(n(1-\alpha)^{1-1/n})$ for the larger particle size with exponents of about 2, implies two-dimensional shrinkage of the reaction interface mechanism. Przepiera *et al.* [29, 30] with a goethite prepared from the oxidative precipitation of aqueous solutions of iron(II) sulphate, obtained activation energy values of between 26–29 kJ mol^{-1} for the goethite dehydroxylation reaction using the Coats–Redfern equation. The mean E value for the studied heating rate range (5, 10 and 20 K min^{-1}) is about 27.6 kJ mol^{-1} and the pre-exponential coefficient equals 49 min^{-1}. The model A_3 has been used as the appropriate equation to describe the goethite dehydroxylation reaction. Walter *et al.* [11] studied the dehydration reaction of a commercial goethite with different particle sizes based on the results obtained in the TG curves, in non-isothermal conditions. They reach E values of between 107.4 and 137.8 kJ mol^{-1}, as a function of the specific surface area and the particle radius. Pelino *et al.* [31] interpreted the decomposition kinetics of goethite according to the shrinking core model for cylindrical particles. The Arrhenius plot of $\ln K$ (kinetic constant) *vs.* $1/T$ yielded activation energy of 119 ± 9 kJ mol^{-1} at 210°C. The R_n model $(n(1-\alpha)^{1-1/n})$ has been used as the appropriate equation to describe the dehydroxylation

reaction of goethite particles with exponents of about 2, implying two-dimensional shrinkage of the reaction interface mechanism. Finally, Fan *et al.* [15] studied the decomposition kinetics of goethite obtained by oxidative precipitation in a sodium bicarbonate medium of a ferrous chloride solution. From the determination of the maximum decomposition grade obtained after calculating T_{max} on the α–T curve, an activation energy value of 112.8 kJ mol^{-1} is reached and a D_3 kinetic model is proposed as the possible mechanism of reaction. The results presented in Fig. 7 clearly show that the decomposition of low-grade nickeliferous laterites ores does not follow a single mechanism because the determined activation energies and pre-exponential factor are not constant during the course of the reaction. The dependence of the kinetic parameters on the reaction extent is clearly visible. This observation indicates that the decomposition of low-grade nickeliferous laterite ores is a complex reaction that cannot be described in terms of a single pair of Arrhenius parameters and commonly used set of reaction models [32].

Conclusions

The application of a simple kinetic model, based on the determination of E, A and $f(\alpha)$, to the dehydroxylation reaction of goethite contained in a low-grade nickeliferous laterites ores yields similar values to those already existing in the literature for goethites obtained by synthetic processes. A two-dimensional shrinkage model of the reaction interface mechanism was adopted as describing the thermal transformation process of goethite from the non-isothermal kinetic analysis. However, this approach is not acceptable for the decomposition reaction of goethite because, as presented in the Friedman analysis plot, the activation energy is often strongly dependent on the reaction progress. The application of simplified kinetics does not allow the correct simulation of the experimental results. In this case, these reactions demonstrate profoundly multi-step characteristics.

References

1 J. A. Batista Rodríguez, Geofís. Internacional, 45 (2006) 39.
2 R. A. B. Bergman, CIM Bull., 96 (2003) 127.
3 A. E. M. Warner, C. M. Díaz, A. D. Dalvi, P. J. Mackey and A. V. Tarasov, JOM, 58 (2006) 11.
4 M. G. King, JOM, 57 (2005) 35.
5 W. P. Imrie, Erzmetall, 59 (2006) 9.
6 D. J. D. C. Kemp, Proc. Int. Conf. Laterite Nickel Symposium. Warrendale, PA:TMS, Charlotte, North Caroline, 2004 p. 45.

7 M. P. Ramírez, 2002. Beneficiabilidad de los escombros
   lateríticos del sector A de la mina de la Pedro Sotto Alba
   Moa Nickel S. A. Tesis ISMM, Moa, p. 61.

8 C. J. Goss, Mineral. Magazine, 51 (1987) 437.

9 A. Manceau and W. P. Gates, Clays Clay Miner.,
   45 (1997) 448.

10 R. G. Ford and P. M. Bertsch, Clays Clay Miner.,
   47 (1999) 329.

11 D. Walter, G. Buxbaum and W. Laqua, J. Therm.
   Anal. Cal., 63 (2001) 733.

12 A. F. Gualtieri and P. Venturelli, Am. Miner., 84 (1999) 895.

13 S. Music, S. Krehula and S. Popovic, Mater. Lett.,
   58 (2004) 444.

14 P. S. R. Prasad, K. Shiva Prasad, V. Krishna Chaitanya,
   E. V. S. S. K. Babu, B. Sreedhar and S. Ramana Murthy,
   J. Asian Earth Sci., 27 (2006) 503.

15 H. Fan, B. Song and Q. Li, Mater. Chem. Phys.,
   98 (2006) 148.

16 J. H. Flynn and L. A. Wall, J. Res. Nat. Bur. Standards,
   70A (1966) 487.

17 T. Ozawa, J. Thermal. Anal., 2 (1970) 301.

18 H. L. Friedman, J. Polym. Sci., 6 (1964) 183.

19 ASTM E698-99. Standard Test Method for Arrhenius
   Kinetic Constants for Thermally Unstable Materials.
   ASTM International. 10-Apr-2001.

20 B. Roduit, C. Borgeat, B. Berger, P. Folly, B. Alonso,
   J. N. Aebischer and F. Stoessel, J. Therm. Anal. Cal.,
   80 (2005) 229.

21 Advanced Kinetics and Technology Software (AKTS) 2006.

22 D. M. Ghodsi and C. Calvo-Roche, J. Therm. Anal. Cal.,
   9 (1976) 435.

23 U. Schwertmann, Thermochim. Acta, 78 (1984) 39.

24 F. Watari, P. Delavignette, V. Landuyt and S. Amelinckx,
   J. Solid State Chem., 48 (1983) 49.

25 O. Ozdemir and D. J. Dunlop, Earth Planetary Sci. Lett.,
   177 (2000) 59.

26 V. Balek and V. J. Subrt, Pure Appl. Chem., 67 (1995) 1839.

27 T. Bellin, N. Guigue, T. Caillot and D. Aymes, J. Solid
   State Chem., 163 (2002) 459.

28 N. Koga, S. Takemoto, T. Nakamura and H. Tanaka,
   Thermochim Acta, 282–283 (1967) 81.

29 K Przepiera and A. Przepiera, J. Therm. Anal. Cal.,
   74 (2003) 659.

30 K. Przepiera and A. Przepiera, J. Therm. Anal. Cal.,
   65 (2001) 497.

31 M. Pelino, L. Toro, M. Petroni, A. Florindi and
   C. Cantalini, J. Mater. Sci., 24 (1989) 409.

32 S. Vyazovkin, J. Therm. Anal. Cal., 83 (2006) 45.